The Astrophysical Journal Supplement Series, 240:25 (7pp), 2019 February https://doi.org/10.3847/1538-4365/aafb12

Experimental Radiative Lifetimes, Branching Fractions, and Oscillator Strengths of Some Levels in Er I and Er II

Qi Yu, Xinghao Wang, Qiu Li, Yongfan Li, and Zhenwen Dai
Key Laboratory of Physics and Technology for Advanced Batteries (Ministry of Education), College of Physics, Jilin University, Changchun 130012, People's Republic of China; dai@jlu.edu.cn
Received 2018 November 8; revised 2018 December 14; accepted 2018 December 22; published 2019 January 31

Abstract

Radiative lifetimes for 104 levels of Erbium (Er) I in the energy range between 31,926.003 and 44,525.705 cm^{-1} and 51 levels of Er II from 31,381.779 to 47,840.962 cm^{-1} were measured by a time-resolved laser-induced fluorescence method. Branching fraction (BF) determinations for 356 lines from 47 out of 104 Er I levels and 122 lines related to 19 out of 51 Er II levels were completed based on the emission spectra of hollow cathode lamps recorded using the 1.0 m Fourier transform spectrometer and are available from the digital library of National Solar Observatory on Kitt Peak, USA (http://diglib.nso.edu/). By combining these BFs and the lifetime results measured in this work, absolute transition probabilities and oscillator strengths were determined for 352 lines of Er I and 92 lines of Er II for the first time, increasing the total number of lines with experimental transition probabilities to over 910 for Er I and over 540 for Er II.

Key words: atomic data – atomic processes – methods: laboratory: atomic – techniques: spectroscopic

Supporting material: machine-readable tables

1. Introduction

Accurate measurements of radiative parameters for rare-earth (RE) atoms and ions are of particular importance in many fields, such as in astronomy, in the lighting-research community, and in theoretical work. In the past few decades, a number of spectral lines of RE atoms and ions have been observed in stellar spectra (Cowley & Mathys 1998; Cowley et al. 2000; Sneden et al. 2003; Johnson & Bolte 2004; Ryabchikova et al. 2006; Ryabchikova & Romanovskaya 2017), which require accurate radiative parameters for the line identifications and abundance determinations. Rich emission spectra in the visible region make RE elements increasingly being used in many commercial metal halide high-intensity discharge lamps. Radiative parameters are needed for modeling and diagnosing these lamps (Biémont & Quinet 2003). RE elements characterized with open 4*f* shells have strong relativistic effects and configuration interaction, making the calculations very difficult. Thus, reliable experimental parameters will be valuable for benchmarking theoretical calculations (Lawler et al. 2008).

Erbium (Er, $Z = 68$) is an RE element observed in the spectra of many stars, such as in AP stars, in AM stars, and in S-type stars (Cowley 1976; Cowley et al. 2000). Over the years, some studies have been focused on acquisition of the radiative parameters for Er I and Er II. For Er I, using the Hartree-plus-statistical exchange approximation, Cowan (1973) computed transition probability values for nine transitions. By means of the absorption method with the atomic beam acting as an absorbent, Dohnalik et al. (1979) measured the absolute values of the oscillator strength for three spectral lines ($\lambda_1 =$ 386.285 nm, $\lambda_2 = 400.797$ nm, and $\lambda_3 = 415.111$ nm). Using the delayed-coincidence method, the lifetimes of 13 excited states in the region 17,074–26,237 cm^{-1} belonging to the $4f^{12}6s6p$ and $4f^{11}5d6s^2$ configurations were measured by Marek & Stahnke (1980). Employing the same method, Gorshkov & Komarovskii (1981) reported 25 lifetimes with energies in the range 19,200–33,485 cm^{-1}. With the model-potential method, which includes both exchange and core polarization, Migdalek & Marcinek (1984) calculated oscillator strengths for $4f^{12}6s^2$–$4f^{12}6s6p$ transitions. With the time-resolved laser-induced fluorescence (TR-LIF) method, Xu et al. (2003a) reported 18 lifetimes for the odd-parity $4f^{12}6s6p$, $4f^{11}5d6s^2$, $4f^{11}5d^26s$, and $4f^{11}5d6s7s$ configurations in the range 26,237–42,154 cm^{-1}. With the same method, the lifetimes of 56 even-parity and 67 odd-parity levels in the range 16,070–40,440 cm^{-1} were measured by Den Hartog et al. (2010). Later, Lawler et al. (2010) reported atomic transition probabilities for 562 lines of Er I with the method of combining branching fractions (BFs) measured using a Fourier transform spectrometer (FTS) with radiative lifetimes reported by Den Hartog et al. (2010).

For Er II, with the beam-foil method, lifetimes of the levels 26,099 and 29,973 cm^{-1} were first reported by Engman et al. (1976). Employing the delayed-coincidence method with crossing atom and electron beams, Gorshkov & Komarovskii (1981) measured lifetimes of 11 levels in the energy range 26,099–31,386 cm^{-1}. Using the same method but with excitation by a collinear tunable dye laser, lifetimes of 11 levels lying in the region 16,643–35,671 cm^{-1} were reported by Bentzen et al. (1982). Using argon–erbium arc plasma, Musiol & Labuz (1983) measured transition probability values for 101 lines. By the means of TR-LIF method, Xu et al. (2003b, 2004) determined lifetimes of 30 odd-parity levels in the energy region 25,592–36,148 cm^{-1} and 8 even-parity levels in the range 33,753–55,317 cm^{-1}, respectively. With the same method, Stockett et al. (2007) measured lifetimes for eight even-parity and 72 odd-parity levels. Later, by combining the BFs measured using an FTS and the lifetime values reported by Stockett et al. (2007), Lawler et al. (2008) determined transition probabilities for 418 lines.

Although many studies on radiative parameters for Er I and Er II have been done in previous work, sufficient data are not available for highly excited levels. Considering the needs in different fields, in the present work, radiative lifetimes of 104 levels for Er I lying in the energy range 31,926.003–44,525.705 cm^{-1} and 51 levels of Er II in the range 31,381.779–47,840.962 cm^{-1} were measured by the TR-LIF method. Meanwhile, the lifetimes of 47 Er I levels and

Table 1
Parameters of the FTS Spectra Used in This Work

Index	Date	Serial Number	Buffer Gas	Lamp Current (mA)	Wavenumber Range (cm^{-1})	Limit of Resolution (cm^{-1})	Beam Splitter	Filter
1	1988 Nov 10	3	Ar	500	7346–42640	0.055	UV	…
2	1988 Nov 11	4	Ar	500	13437–4264	0.055	UV	$CuSO_4$
3	1987 Jan 13	5	Ar	500	3488–15077	0.029	Vis	…
4	2000 Feb 28	32	Ar	26.5	7929–34998	0.053	UV	…
5	2002 Feb 26	10	Ar	27	7929–34998	0.050	UV	…
6	2000 Feb 28	27	Ar	26.5	7929–34998	0.053	UV	…
7	2000 Feb 28	26	Ar	23	7929–34998	0.053	UV	…
8	2000 Feb 28	28	Ar	17	7929–34998	0.053	UV	…

Note. All spectra are publicly available from the digital library of the NSO on Kitt Peak, USA (http://diglib.nso.edu/).

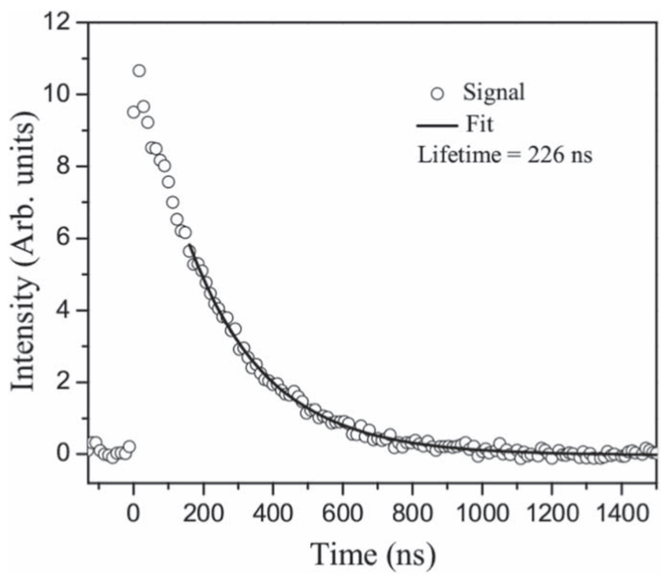

Figure 1. Fluorescence decay curve of the Er I level 35,601.377 cm^{-1} with an exponential fit.

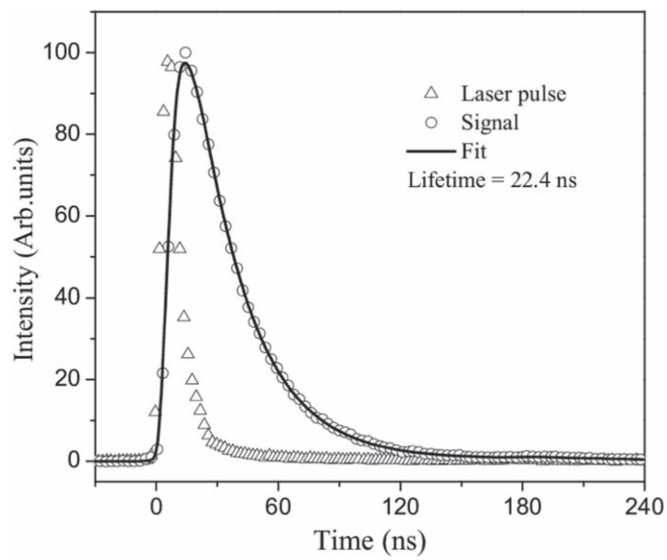

Figure 2. Typical fluorescence decay curve of the Er I level 38,667.799 cm^{-1} with the fitted convolution curve between the laser pulse and an exponential.

19 Er II levels reported in this work were combined with BFs determined based on the spectra recorded using an FTS to derive transition probabilities (gA) and oscillator strengths ($\log(gf)$) for 356 lines in Er I levels and 122 lines related to Er II levels.

2. Lifetime Measurements

Since the experimental setup was recently presented in detail by Tian et al. (2016), here we only give a brief description. Free neutral and singly ionized Er in their ground and low-lying metastable levels were produced by focusing laser pulses vertically onto the surface of a rotating Er target placed inside a vacuum chamber with the pressure of about 10^{-4}–10^{-3} Pa. The laser pulses are emitted from a 532 nm Q-switched Nd:YAG laser operating at 10 Hz with an energy of 5–10 mJ. In order to excite Er I and Er II to the investigated states, another Nd:YAG 532 nm laser was used to pump a dye laser (DCM or Rhodamine 6G dyes), which was followed by different nonlinear processes to obtain tunable excitation source. Then the excitation laser was horizontally sent into the vacuum chamber to intersect with the Er atoms and ions at the distance of about 8 mm above the target surface. The two pump lasers were triggered by a digital delay generator (SRS DG535), which can also freely adjust the delay time between them. Fluorescence from the measured levels was collected by a

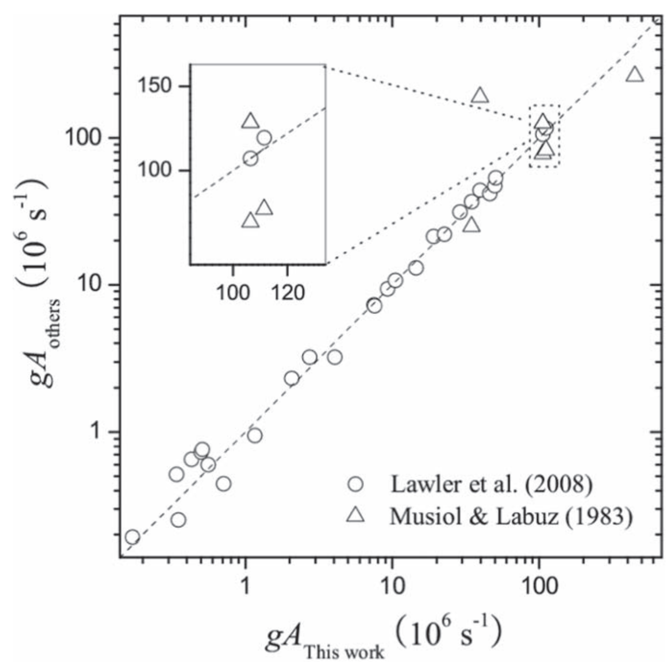

Figure 3. Comparisons between the Er II gA values in this work, by Lawler et al. (2008), and by Musiol & Labuz (1983). The dashed line corresponds to the equality between our results and the others.

Table 2
Measured Lifetimes of Er I Levels and Comparison with Previous Results

Upper Level[a]			Lower Level[a]		$\lambda_{Exc.}$	$\lambda_{Obs.}$	Lifetime (ns)	
Config.	J	E (cm^{-1})	J	E (cm^{-1})	(nm)	(nm)	This Work	Previous
	6	31926.003	6	0.000	313.224	400	109(6)	106(5)[b], 105(10)[c]
	3	31988.938	4	5035.193	371.006	371	493(14)	
$4f^{11}(^4F°)5d6s^2$	3	32695.370	4	5035.193	361.531	456	111(2)	
	8	34288.437	7	7696.956	376.060	401	80.0(56)	
	7	34596.396	7	7696.956	371.755	434	86.3(78)	
	5	34684.329	6	0.000	288.315	361	44.6(21)	42.6(21)[b], 45(4)[c]
	8	34756.580	7	7696.956	369.554	394	102(4)	
	7	35191.459	7	7696.956	363.709	497	130(6)	
	6	35218.609	7	7696.956	363.350	420	66.9(51)	
	8	35300.412	7	7696.956	362.273	404	42.1(40)	
	5	35328.671	6	7176.503	355.212	418	213(13)	
	9	35402.733	9	8620.565	373.383	419	201(13)	
	8	35493.301	9	8620.565	372.124	401	58.5(47)	
	3	35585.434	4	5035.193	327.330	403	17.7(3)	
$4f^{12}(^1G)6s6p(^3P°)$	4	35601.377	4	5035.193	327.159	402	226(4)	
$4f^{11}(^2K°)5d6s^2$	6	35632.524	6	0.000	280.642	349	194(2)	190(10)[c]
	4	35783.707	4	5035.193	325.219	399	153(4)	
$4f^{12}(^1G)6s6p(^3P°)$	3	35818.334	4	5035.193	324.853	399	158(2)	
	7	35833.788	8	9350.106	377.591	482	22.7(6)	
	6	35918.454	7	7696.956	354.340	482	75.8(53)	
	6	35963.366	7	7696.956	353.777	414	59.1(37)	
	6	36026.864	7	7696.956	352.984	480	70.6(38)	
	4	36280.029	4	5035.193	320.053	392	31.5(17)	
	5	36287.081	4	5035.193	319.981	392	484(6)	
	7	36418.402	8	9350.106	369.436	469	30.3(6)	
	4	36431.169	4	5035.193	318.512	389	31.4(15)	
	5	36465.938	4	5035.193	318.160	389	201(4)	
	4	36747.783	4	5035.193	315.332	385	264(5)	
$4f^{11}(^4G°)5d6s^2$	3	36930.659	4	5035.193	313.524	382	14.0(3)	
$4f^{11}(^4I°)5d^2(^3F)$ $(^4F°)6s$	3	37075.570	4	5035.193	312.106	380	178(4)	
	4	37083.198	4	5035.193	312.032	380	123(3)	
$4f^{12}(^1G)6s6p(^3P°)$	3	37125.206	4	5035.193	311.623	404	36.8(8)	
	4	37210.947	4	5035.193	310.793	378	73.9(32)	
	4	37265.129	4	5035.193	310.271	402	115(2)	
	3	37289.592	4	5035.193	310.035	401	17.8(4)	
	4	37319.434	4	5035.193	309.749	401	268(2)	
	5	37398.878	5	6958.329	328.509	375	157(7)	
	5	37535.325	4	5035.193	307.691	373	95.3(9)	
	6	37542.792	6	7176.503	329.313	383	84.3(26)	
	4	37582.298	4	5035.193	307.247	373	127(3)	
	3	37649.344	4	5035.193	306.615	396	107(2)	
	7	37714.613	6	7176.503	327.460	353	11.0(3)	
	5	37778.256	4	5035.193	305.408	370	251(5)	
	7	37806.983	6	7176.503	326.472	351	93.0(22)	
	4	37853.673	5	6958.329	323.673	393	73.1(72)	
	4	37970.621	5	6958.329	322.453	391	14.2(9)	
	7	38195.326	6	7176.503	322.385	347	96.9(45)	
	8	38253.685	7	7696.956	327.260	361	27.9(17)	
	7	38301.613	6	7176.503	321.284	345	29.1(19)	
$4f^{12}(^3H)6s6d$?	6	38407.470	7	7696.956	325.621	453	16.2(8)	
	6	38547.832	6	7176.503	319.680	375	63.7(40)	
	6	38604.588	7	7696.956	323.545	368	110(3)	
	7	38664.249	6	7176.503	317.584	369	37.7(9)	
$4f^{12}(^3H)6s6d$?	6	38667.799	6	7176.503	317.548	372	22.4(13)	
	5	38703.037	6	7176.503	317.193	372	21.1(13)	
	8	38734.243	7	7696.956	322.193	355	20.9(11)	
$4f^{12}(^3H)6s6d$?	7	38751.622	6	7176.503	316.705	461	19.9(8)	
	6	38786.542	6	7176.503	316.355	371	50.7(33)	
$4f^{12}(^3H)6s6d$?	5	38795.477	6	7176.503	316.266	365	19.2(4)	
$4f^{12}(^3H)6s6d$?	7	38797.084	6	7176.503	316.250	436	18.1(6)	
	7	38857.639	7	7696.956	320.917	370	146(5)	
$4f^{12}(^3H_5)6s7s(^3S_1)$	6	38870.770	7	7696.956	320.782	371	41.2(27)	
$4f^{12}(^3H)6s6d$?	6	38923.586	6	7176.503	314.990	363	62.2(32)	

Table 2
(Continued)

Upper Level[a]			Lower Level[a]		$\lambda_{Exc.}$	$\lambda_{Obs.}$	Lifetime (ns)	
Config.	J	E (cm^{-1})	J	E (cm^{-1})	(nm)	(nm)	This Work	Previous
	4	38982.003	5	6958.329	312.269	257	90.9(14)	
	7	38986.765	6	7176.503	314.364	368	32.2(10)	
	6	39010.445	7	7696.956	319.351	455	22.2(4)	
$4f^{12}(^3H)6s6d$?	7	39070.645	7	7696.956	318.738	368	33.5(6)	
	6	39075.883	6	7176.503	313.486	361	19.4(7)	
	7	39145.450	6	7176.503	312.804	362	22.0(4)	
	6	39164.268	6	7176.503	312.620	365	124(3)	
$4f^{12}(^3H)6s6d$?	6	39193.564	6	7176.503	312.333	365	23.6(14)	
	6	39256.456	7	7696.956	316.862	364	33.9(12)	
	6	39350.505	6	7176.503	310.810	363	8.2(3)	
	7	39359.683	6	7176.503	310.721	360	4.8(2)	
	8	39525.603	7	7696.956	314.182	362	18.5(5)	
	6	39535.919	5	6958.329	306.959	253	37.1(7)	
	3	39688.151	4	5035.193	288.576	376	121(2)	
	5	39812.042	6	7176.503	306.414	357	55.6(41)	
	8	39843.429	7	7696.956	311.076	354	17.7(5)	
	7	40131.326	8	9350.106	324.873	354	29.7(29)	
	7	40159.218	7	7696.956	308.050	354	20.8(16)	
	6	40333.576	7	7696.956	306.404	352	29.4(23)	
	7	41269.956	8	9350.106	313.285	393	14.0(2)	
	7	41809.765	8	9350.106	308.075	385	24.5(16)	
	6	41907.318	6	7176.503	287.929	374	29.6(25)	
	7	41989.925	8	11557.670	328.599	383	48.3(36)	
	5	42360.935	6	7176.503	284.217	384	21.0(10)	
	8	42376.272	7	7696.956	288.356	459	12.7(11)	
	5	42542.173	6	7176.503	282.760	366	15.7(7)	
	6	42627.566	6	11799.778	324.383	373	46.7(26)	
$4f^{12}(^3H_4)6s7s(^3S_1)$	5	42736.803	6	7176.503	281.212	375	19.7(29)	
	8	42797.550	7	7696.956	284.895	361	6.3(4)	
	6	42882.350	6	7176.503	280.066	388	10.6(4)	
	6	43191.617	7	11887.503	319.447	366	18.6(6)	
	6	43298.210	7	7696.956	280.889	356	6.3(3)	
	8	43537.586	7	7696.956	279.013	370	11.0(4)	
	8	43586.058	9	8620.565	285.996	351	8.9(3)	
	9	43982.879	9	8620.565	282.787	364	13.8(11)	
	7	44039.685	8	9350.106	288.271	355	14.7(4)	
	8	44041.430	9	8620.565	282.319	372	8.9(9)	
	10	44112.202	9	8620.565	281.757	362	11.7(4)	
	8	44201.047	9	8620.565	281.053	387	13.2(4)	
	7	44394.215	8	9350.106	285.355	384	12.3(3)	
	9	44525.705	8	9350.106	284.288	357	11.2(5)	

Notes.
[a] Kramida et al. (2018).
[b] Den Hartog et al. (2010).
[c] Xu et al. (2003a).

fused-silica lens in the direction perpendicular to the two laser beams and focused into a monochromator, equipped with a photomultiplier tube to convert the fluorescence into an electric signal. Then the signal was sent to a digital oscilloscope (Tektronix DPO7254) for recording.

In the measurements, by monitoring the wavelength of the dye laser through a high-precision wavemeter (HighFinesse WS6) and by checking the fluorescence wavelengths, we made sure only investigated Er I and Er II levels were excited. Beside that, all possible effects, such as the saturation, collision, radiation trapping, and flight-out-of-view effects, which can influence lifetime measurements, were minimized via modifications of experimental conditions (Wang et al. 2018). A magnetic field, about 100 Gauss, was added over the plasma zone by a pair of Helmhotz coils to eliminate possible quantum beats caused by the Earth's magnetic field. During the measurements, an average of more than 1000 pulses was performed to improve the signal-to-noise ratio of each signal.

3. BF Determinations

For determination of BFs for all Er I and Er II levels whose lifetimes were measured in this work, we attempted to observe emission spectra of an Er hollow cathode lamp with our grating spectrometer (Acton SpectraPro500i), but too many of the investigated lines overlap with other Er I and Er II lines so that

Table 3
Measured Lifetimes of Er II Levels and Comparison with Previous Results

Upper Level[a]			Lower Level[a]		$\lambda_{\mathrm{Exc.}}$	$\lambda_{\mathrm{Obs.}}$	Lifetime (ns)	
Config.	J	E(cm^{-1})	J	E(cm^{-1})	(nm)	(nm)	This Work	Previous
	9/2	31381.779	11/2	440.434	323.192	381	298(11)	
	11/2	31801.102	11/2	440.434	318.871	406	127(4)	126(6)[b]
	7/2	31902.682	9/2	5132.608	373.551	374	113(4)	
	11/2	32073.360	11/2	440.434	316.126	401	105(5)	101(5)[b],102(10)[c],104(10)[d]
	9/2	32267.246	11/2	440.434	314.200	369	50.1(27)	45.9(23)[b],49(3)[c]
	11/2	32618.753	11/2	440.434	310.768	364	75.7(38)	73.4(37)[b],75(3)[c]
	9/2	32753.468	11/2	440.434	309.473	391	124(2)	
	7/2	32790.085	9/2	5132.608	361.566	365	58.8(33)	
	11/2	32811.006	11/2	440.434	308.923	361	74.0(53)	72.4(36)[b]
$4f^{11}(^4I^{\circ}_{15/2})6s6p(^3P^{\circ}_1)$	17/2	33217.200	15/2	6824.774	378.897	490	26.5(8)	
$4f^{11}(^4I^{\circ}_{15/2})6s6p(^3P^{\circ}_1)$	15/2	33547.268	15/2	6824.774	374.217	487	30.0(6)	
	7/2	34203.251	9/2	7195.355	370.262	370	154(8)	
	13/2	35276.531	11/2	440.434	287.059	356	136(3)	144(7)[b]
	9/2	35877.083	7/2	5403.688	328.155	400	306(9)	
	11/2	35885.232	11/2	440.434	282.129	348	174(6)	
	9/2	36322.233	7/2	5403.688	323.430	393	111(3)	
	7/2	36471.984	9/2	5132.608	319.087	391	121(9)	
	11/2	36643.232	9/2	5132.608	317.353	339	29.1(8)	
	7/2	36738.247	7/2	5403.688	319.136	389	14.4(8)	
	11/2	36863.932	9/2	5132.608	315.146	337	78.6(41)	
	9/2	37038.764	9/2	5132.608	313.419	382	69.0(45)	
	7/2	37057.724	9/2	5132.608	313.233	384	32.6(19)	
	11/2	37098.956	9/2	5132.608	312.829	334	90.0(40)	
	5/2	37126.953	7/2	5403.688	315.226	408	56.3(25)	
	7/2	37527.159	7/2	5403.688	311.299	375	130(5)	
	7/2	37698.823	7/2	5403.688	309.644	373	27.7(18)	
	5/2	37712.008	7/2	5403.688	309.518	398	64.4(52)	
	11/2	38642.554	11/2	7149.630	317.532	362	56.0(33)	
	7/2	38651.814	9/2	7195.355	317.900	362	20.3(7)	
	9/2	38847.186	11/2	7149.630	315.482	358	53.5(44)	
$4f^{11}(^4I^{\circ})6s6p$?	13/2	38847.378	15/2	6824.774	312.279	363	15.8(7)	
	7/2	39140.561	9/2	7195.355	313.036	377	88.6(38)	
	11/2	39242.082	11/2	7149.630	311.600	355	76.6(41)	
	7/2	39304.952	9/2	7195.355	311.433	354	68.2(61)	
	9/2	39392.224	11/2	7149.630	310.149	353	91.4(48)	
	9/2	39509.332	11/2	7149.630	309.026	371	65.5(63)	
	9/2	39653.816	11/2	7149.630	307.653	348	81.2(49)	
	9/2	39845.276	9/2	5132.608	288.079	345	57.9(35)	
	7/2	39975.403	9/2	5132.608	287.003	346	61.2(43)	
	9/2	40000.774	9/2	5132.608	286.795	345	27.7(27)	
	5/2	40123.804	7/2	5403.688	288.017	342	17.5(6)	
	11/2	40435.615	9/2	5132.608	283.262	300	69.4(35)	
	7/2	40747.134	7/2	5403.688	282.938	413	124(6)	
	9/2	40905.867	7/2	5403.688	281.673	335	25.1(24)	
	7/2	40943.527	9/2	5132.608	279.244	334	25.4(16)	
	9/2	40959.837	9/2	5132.608	279.117	333	64.1(42)	
	9/2	41067.403	7/2	5403.688	280.397	331	18.5(5)	
	9/2	41170.514	7/2	5403.688	279.589	330	29.5(16)	
	7/2	41206.903	7/2	5403.688	279.305	349	64.2(30)	
	7/2	41876.127	9/2	7195.355	288.344	324	32.6(7)	
	13/2	47840.962	11/2	12388.090	282.065	359	125(7)	

Notes.
[a] Kramida et al. (2018).
[b] Stockett et al. (2007).
[c] Xu et al. (2003b).

BF measurements cannot be performed. However, it is possible to determine BFs using the FTS spectra available from the digital library of the National Solar Observatory (NSO) on Kitt Peak, USA (http://diglib.nso.edu/). The NSO FTS, characterized with very high resolving power and excellent absolute wavenumber accuracy, has been used in BF measurements for

Table 4
Branching Fractions (R_{ki}), Transition Probabilities, Oscillator Strengths of Er I Levels, and Comparison with Previous Results

Upper level[a]				Lower level[a]		Transition	R_{ki}	$g_kA_{ki}(10^6\ \mathrm{s}^{-1})$		$\mathrm{Log}(g_if_{ik})$	
Config.	J	E_k (cm^{-1})	τ (ns)	J	E_i (cm^{-1})	λ_{air} (nm)[b]		This Work	Previous[c]	This Work	Previous[c]
	6	31926.003	109(6)	5	6958.329	400.405	1.00(0)	119(7)	120(7)	−0.54(2)	−0.54
	3	31988.938	493(14)	4	5035.193	370.900	0.906(7)	12.9(4)		−1.58(1)	
				4	10750.982	470.723	0.033(4)	0.467(56)		−2.81(5)	
				3	12377.534	509.765	0.034(4)	0.486(65)		−2.72(6)	
				2	13097.906	529.205	0.027(4)	0.378(62)		−2.80(7)	
$4f^{11}(^4F^\circ)5d6s^2$	3	32695.370	111(2)	4	5035.193	361.428	0.079(12)	5.00(79)		−2.01(7)	
				4	10750.982	455.569	0.842(13)	53.5(13)		−0.78(1)	
				3	12377.534	492.041	0.050(6)	3.16(37)		−1.94(5)	
				2	13097.906	510.128	0.024(4)	1.51(27)		−2.23(8)	
				4	23300.042	1064.067	0.005(1)	0.29(8)		−2.30(12)	

Notes.
[a] Kramida et al. (2018).
[b] Wavelength values computed from energy levels using the five-parameter formular from Peck & Reeder (1972).
[c] Lawler et al. (2010).

(This table is available in its entirety in machine-readable form.)

Table 5
Branching Fractions (R_{ki}), Transition Probabilities, Oscillator Strengths of Er II Levels, and Comparison with Previous Results

Upper Level[a]			τ (ns)	Lower Level[a]		Transition (nm)[b]	R_{ki}	g_kA_{ki} $(10^6\ \mathrm{s}^{-1})$		$\mathrm{Log}(g_if_{ik})$	
Config.	J	E_k (cm^{-1})		J	E_i (cm^{-1})	λ_{air}		This Work	Previous[c]	This Work	Previous
	11/2	31801.102	127(4)	13/2	0.000	314.364	0.239(7)	22.6(10)	22.1(12)	−1.48(2)	−1.49
				11/2	440.434	318.779	0.366(10)	34.6(14)	36.8(19),25(12)[d]	−1.28(2)	−1.25
				9/2	5132.608	374.867	0.079(5)	7.49(51)	7.32(60)	−1.80(3)	−1.81
				11/2	7149.630	405.540	0.153(15)	14.5(8)	13.0(11)	−1.45(4)	−1.50
				9/2	7195.355	406.294	0.111(8)	10.5(8)	10.7(10)	−1.58(3)	−1.58
				9/2	11042.640	481.596	0.002(1)	0.170(30)	0.192(36)	−3.22(8)	−3.17
				9/2	16552.871	655.633	0.029(6)	2.73(58)	3.24(72)	−1.76(9)	−1.68
				11/2	18889.101	774.260	0.004(1)	0.340(80)	0.516(132)	−2.51(10)	−2.33
				11/2	21697.852	989.510	0.007(2)	0.660(170)	0.444(108)	−1.98(10)	−2.18
				9/2	21894.055	1009.106	0.004(1)	0.350(80)	0.252(60)	−2.28(10)	−2.41

Notes.
[a] Kramida et al. (2018).
[b] Wavelength values computed from energy levels using the five-parameter formula from Peck & Reeder (1972).
[c] The values not labeled were measured by Lawler et al. (2008).
[d] Musiol & Labuz (1983).

(This table is available in its entirety in machine-readable form.)

some atoms and ions (see e.g., Den Hartog et al. 2015; Lawler et al. 2017; Li et al. 2018). Table 1 is a list of eight FTS spectra from the NSO used in our BF study.

For the NSO FTS spectra, accurate calibration of spectral response is indispensable because the instrument system has different responses at different wavelengths. We made used of the Ar I and Ar II line calibrations, which is based on comparison of the high-precision branching ratios for Ar I and Ar II lines (Hashiguchi & Hasikuni 1985; Whaling et al. 1993) to the intensity ratios measured for the same lines to obtain the spectral response. As indicated in Table 1, the set of eight spectra used in this study including both high-current spectra to reveal extremely weak lines and low-current spectra, which can avoid the reabsorption effect characterized by a suppression of the strong emission line and the weak emission lines enhancements (Lawler et al. 2010). In the present work, by comparing BF results from spectra at different currents, we checked whether the reabsorption effect exists or not. If it exists, only the spectra at low currents were used. Considering possible blends from spectral lines of Er and carrier Ar gas, we carefully distinguished the measured Er lines to make sure that the investigated lines were correctly assigned.

4. Results and Discussion

In the lifetime measurements, for the lifetimes longer than 40 ns, which correspond to five times the exciting pulse duration, the lifetime values were evaluated by fitting the recorded fluorescence curve to an exponential function with adjustable parameters. Otherwise, due to limitation of the excitation pulse duration and the response time of the detection system, a convolution fit of an exponential and an exciting pulse recorded by the same system to the decay curves is necessary for extracting lifetime values. As examples, a fluorescence curve of the Er I level 35,601.377 cm^{-1} with an exponential fit is shown in Figure 1, while the decay curve of the Er I level 38667.799 cm^{-1}, the recorded excitation pulse and a convolution, are presented in Figure 2.

The radiative lifetimes of 104 levels in Er I lying in the energy range 31,926.003–44,525.705 cm^{-1} and of 51 levels of Er II lying in the range 31,381.779–47,840.962 cm^{-1} were determined and are listed in Tables 2 and 3, respectively, with quoted error bars, which consist of possible remaining systematic errors and statistical scattering errors from different recordings. The measured results are in a range of 4.8 to 493 ns, with uncertainties within 10%, except for the Er I levels 42,736.803 and 44,041.43 cm^{-1} that have uncertainties of 14.7% and 10.1%, respectively. To our best knowledge, the lifetimes for 101 out of 104 levels in Er I and for 45 out of 51 levels in Er II were measured for the first time. Also included in the final columns of Tables 2 and 3 are some lifetime results from previous literature. We see good agreements between our and previous results with the differences, with ours as the reference ((ours-theirs)/ours), within ±10%.

The BFs were determined from line intensities divided by spectral response values. The BF uncertainties consist of two components: the line intensity errors and the calibration errors. The former were estimated using an analytical function of the signal-to-noise ratio, the FWHM of line, and the resolution interval of the spectrum (Sikström et al. 2002), while the latter were evaluated as 1% per 1000 wavenumber separation between the line of interest and the dominant line from the upper level (Wickliffe et al. 2000). The total uncertainty of the BF was calculated by the error-propagation theory (Sikström et al. 2002). We would like to deduce BFs for all Er levels measured in our lifetime experiment, but because the investigated levels have branches beyond the ultraviolet (UV) limit of the FTS spectra or they have one or more strong branches with a possibly severe blending problem, the BFs can be determined only for 47 Er I and 19 Er II levels.

BFs were combined with the measured lifetimes to determine gA and $\log(gf)$ for which the uncertainties were evaluated by the error transfer theory (Sikström et al. 2002). The BFs, as well as the deduced gA and $\log(gf)$, concerning Er I and Er II levels are listed in Tables 4 and 5, respectively. In these tables, we also present the previous results measured by Lawler et al. (2010), Musiol & Labuz (1983), and Lawler et al. (2008) for comparisons. For the gA values of Er I, good agreements can be seen between us and Lawler et al. (2010). The differences are less than ±6.6% for three lines and 21.7% for the weak line 337.181 nm (BF $R_{ki} = 0.038$).

Figure 3 is a comparison of our Er II gA results to those reported by Musiol & Labuz (1983) and by Lawler et al. (2008). We see, for the strong lines with gA values greater than $10^6\ s^{-1}$, good agreements between our results and those by Lawler et al. (2008). A little larger discrepancies appear when comparing the gA values by Musiol & Labuz (1983) with our results. The similar situation also occurs in the comparisons between the gA values by Lawler et al. (2008) and by Musiol & Labuz (1983). Incorrect line identifications in the measurements by Musiol & Labuz (1983) may be responsible for the deviations because the earlier grating spectrometer used by Musiol & Labuz had a lower resolving power and cannot be competent to analyze the complex Er spectra.

In conclusion, radiative lifetimes for 104 levels of Er I in the energy range 31,926.003–44,525.705 cm^{-1} and 51 levels of Er II in the range 31,381.779–47,840.962 cm^{-1} were measured by the TR-LIF method. To the best of our knowledge, the lifetimes for 101 out of 104 levels in Er I and for 45 out of 51 levels in Er II were measured for the first time. BFs for 356 Er I lines and 122 Er II lines from the levels for which the lifetimes were studied in the present work were determined based on the FTS spectra from the digital library of the NSO on Kitt Peak, USA. By combining the BF and the lifetime results, the experimental gA and $\log(gf)$ for these transitions were derived.

This work was supported by the National Natural Science Foundation of China (grant No. U1832114) and by the Science and Technology Development Planning Project of Jilin Province (grant No. 20180101239JC).

ORCID iDs

Zhenwen Dai https://orcid.org/0000-0002-9040-2315

References

Bentzen, S. M., Nielsen, U., & Poulsen, O. 1982, JOSA, 72, 1210
Biémont, E., & Quinet, P. 2003, PhST, 105, 38
Cowan, R. D. 1973, NucIM, 110, 173
Cowley, C. R. 1976, ApJS, 32, 631
Cowley, C. R., & Mathys, G. 1998, A&A, 339, 165
Cowley, C. R., Ryabchikova, T., Kupka, F., et al. 2000, MNRAS, 317, 299
Den Hartog, E. A., Chisholm, J. P., & Lawler, J. E. 2010, JPhB, 43, 155004
Den Hartog, E. A., Palmer, A. J., & Lawler, J. E. 2015, JPhB, 48, 155001
Dohnalik, A., Dohnalik, T., & Szynarowska, M. 1979, PhyS, 20, 39
Engman, B., Stoner, J. O., Martinson., I., & Cerne, N. E. 1976, PhyS, 13, 363
Gorshkov, V. N., & Komarovskii, V. A. 1981, OptSp, 50, 467
Hashiguchi, S., & Hasikuni, M. 1985, JPSJ, 54, 1290
Johnson, J. A., & Bolte, M. 2004, ApJ, 605, 462
Kramida, A., Ralchenko, Y., Reader, J. & NIST ASD Team 2018, NIST Atomic Spectra Database (ver. 5.5.6), https://physics.nist.gov/asd
Lawler, J. E., Sneden, C., Cowan, J. J., et al. 2008, ApJS, 178, 71
Lawler, J. E., Sneden, C., Nave, G., et al. 2017, ApJS, 228, 10
Lawler, J. E., Wyart, J. F., & Den Hartog, E. A. 2010, JPhB, 43, 235001
Li, Q., Yu, Q., Wang, X. H., et al. 2018, JOSAB, 35, 2244
Marek, J., & Stahnke, H. J. 1980, ZPhyA, 298, 81
Migdalek, J., & Marcinek, R. 1984, JQSRT, 32, 269
Musiol, K., & Labuz, S. 1983, PhyS, 27, 422
Peck, E. R., & Reeder, K. 1972, JOSA, 62, 958
Ryabchikova, T. A., & Romanovskaya, A. M. 2017, AstL, 43, 252
Ryabchikova, T. A., Ryabtsev, A., Kochukhov, O., & Bagnulo, S. 2006, A&A, 456, 329
Sikström, C. M., Nilsson, H., Litzén, U., Blom, A., & Lundberg, H. 2002, JQSRT, 74, 355
Sneden, C., Cowan, J. J., Lawler, J. E., et al. 2003, ApJ, 591, 936
Stockett, M. H., Den Hartog, E. A., & Lawler, J. E. 2007, JPhB, 40, 4529
Tian, Y. S., Wang, X. H., Yu, Q., et al. 2016, MNRAS, 457, 1393
Wang, X. H., Quinet, P., Li, Q., et al. 2018, JQSRT, 212, 112
Whaling, W., Carle, M. T., & Pitt, M. L. 1993, JQSRT, 50, 7
Wickliffe, M. E., Lawler, J. E., & Nave, G. 2000, JQSRT, 66, 363
Xu, H. L., Jiang, H. M., Liu, Q., Jiang, Z. K., & Svanberg, S. 2004, ChPhL, 21, 1720
Xu, H. L., Jiang, Z., & Svanberg, S. 2003a, PhyS, 67, 64
Xu, H. L., Jiang, Z. K., Zhang, Z. G., et al. 2003b, JPhB, 36, 1771